# Microheterogeneity of Actin Gels Formed under Controlled Linear Shear

Jorge Daniel Cortese and Carl Frieden

Department of Biological Chemistry, Division of Biological and Biomedical Sciences, Washington University School of Medicine, St. Louis, Missouri 63110

*Abstract.* The diffusion coefficients and fluorescence polarization properties of actin subjected to a known shear have been determined both during and after polymerization, using a modification of a cone-plate Wells-Brookfield rheometer that allows monitoring of samples with an epifluorescence microscope. Fluorescence polarization and fluorescence photobleaching recovery experiments using rhodamine-labeled actin as a tracer showed that under conditions of low shear (shear rates of 0.05 s$^{-1}$), a spatial heterogeneity of polymerized actin was observed with respect to fluorescence intensity and the diffusion coefficients with actin mobility becoming quite variable in different regions of the sample. In addition, complex changes in fluorescence polarization were noted after stopping the shear. Actin filaments of controlled length were obtained using plasma gelsolin (gelsolin/actin molar ratios of 1:50 to 1:300). At ratios of 1:50, neither spatial heterogeneity nor changes in polarization were observed on subjecting the polymerized actin to shear. At ratios of ∼1:100, a decrease on the intensity of fluorescence polarization occurs on stopping the shear. Longer filaments exhibit spatial microheterogeneity and complex changes in fluorescence polarization. In addition, at ratios of 1:100 or 1:300, the diffusion coefficient decreases as the total applied shear increased. This behavior is interpreted as bundling of filaments aligned under shear. We also find that the F-actin translational diffusion coefficients decrease as the total applied shear increases (shear rates between 0.05 and 12.66 s$^{-1}$), as expected for a cumulative process. When chicken gizzard filamin was added to gelsolin-actin filaments (at filamin/actin molar ratios of 1:300 to 1:10), a similar decrease in the diffusion coefficients was observed for unsheared samples. Spatial microheterogeneity might be related to the effects of the shear field in the alignment of filaments, and the balance between a three-dimensional network and a microheterogeneous system (containing bundles or anisotropic phases) appears related to both shear and the presence of actin-binding proteins.

A complex sol–gel transition of components of the cell cytoplasm could be important for variations in cell shape and its biomechanical functions. The understanding of the rheological properties of the cortical cytoplasm should be then the first step toward a serious study of many aspects of cytoskeletal biomechanics (Stossel, 1986; Stossel et al., 1987; Elson, 1988). We have undertaken such an effort by simulating in vitro mechanical properties of cytoplasm using the purified components (i.e., actin and actin-binding proteins) to grow actin filaments of controlled length and different degrees of association. This study investigates the effect of controlled shear on these filaments. To examine the response of actin gels to shear, we have redesigned a cone and plate rheometer for use in conjunction with an epifluorescence microscope and measured translational diffusion coefficients, filament mobility (by fluorescence photobleaching recovery [FPR][1]), or fluorescence polarization after a known homogeneous shear is applied.

We report here that shear induces microheterogeneity in actin gels, probably by side-to-side filament–filament association into larger aggregates or bundles. The partial orientation of filaments that grow under a shear field eliminates, to some extent, topological constraints for interaction between them, and filament–filament association arises spontaneously under these conditions. In addition, we have investigated the effect on this association of actin-binding proteins that regulate filament length (gelsolin), and that induce interaction between filaments (filamin). The approach used provides new insights about the viscoelastic behavior of actin and its dynamics, and suggests important effects of shear in cytoskeletal organization and actin dynamics.

---

1. *Abbreviations used in this paper:* F/A, molar ratio of monomeric filamin (mol wt = 250,000) to actin (unpolymerized or polymerized as filaments);

FPR, fluorescence photobleaching recovery technique; G/A, molar ratio of plasma gelsolin (mol wt = 82,000) to actin (unpolymerized or polymerized as filaments).

## Materials and Methods

### Reagents

ATP (disodium salt grade I), β-mercaptoethanol, dithioerythritol, dithiothreitol (DTT), EDTA, EGTA and tris(hydroxy-methyl)aminomethane (Tris) were purchased from Sigma Chemical Co. (St. Louis, MO). DEAE-Sepharose 6B, Sephacryl S-400, and Sephadex G-150 were obtained from Pharmacia Fine Chemicals (Uppsala, Sweden). Ion exchangers DE-52 and PL-11 (phosphocellulose in a fiber form) were obtained from Whatman Inc. (Clifton, NJ). A mixture of isomers of (iodoacetamido) tetramethylrhodamine (MW 569.5) was purchased from Research Organics, Inc. (Cleveland, OH). CaCl₂ (Puritronic) and "ultrapure" MgSO₄ were obtained from Alfa Products, Thiokol/Ventron Division (Danvers, MA). All the other reagents were of analytical grade, and double distilled water was used in all the experiments.

### Protein Purification

Actin was prepared from rabbit skeletal muscle, as previously described (Tait and Frieden, 1982a), according to the procedure of Spudich and Watt (1971), and with the gel filtration step described by MacLean-Fletcher and Pollard (1980). Actin was stored at −20°C as a lyophilized mixture with sucrose (2 mg of sucrose per 1 mg of actin; Tellam and Frieden, 1982). Lyophilized actin was dissolved (total actin concentration of 2–5 mg/ml) and dialyzed at 4°C for 1–2 d against G-buffer (0.2 mM CaCl₂, 1.5 mM NaN₃, 0.2 mM ATP, 2 mM Tris-HCl, pH 8.0) before use.

Rhodamine-labeled actin was prepared using (iodoacetamido)tetramethylrhodamine as described by Tait and Frieden (1982a). The labeled material contained 0.5–0.6/mol of rhodamine per mol of total protein. Actin and rhodamine-labeled actin concentrations were estimated by the method of Bradford (1976), using actin as a standard. The extinction coefficient at 290 nm and 1-cm light path is $E^{1\ mg/ml} = 0.63$ (Houk and Ue, 1974).

Plasma gelsolin (or brevin) was prepared from rabbit plasma (Pel-Freez Biologicals, Rogers, AR) using a procedure based on that of Cooper et al. (1987). These authors combined early methods for brevin isolation of Soua et al. (1985) and Chaponnier et al. (1985). The rabbit plasma is extracted in 25 mM Tris-HCl, pH 7.5, containing 0.1 mM phenylmethylsulfonyl fluoride (PMSF) and 25 mM CaCl₂ for 30 min at 37°C, to allow clot retraction. After two successive steps of ammonium sulfate fractionation (25 and 50%), the final pellet is dialyzed against a buffer containing 10 mM Tris-HCl, pH 8.0, 1.5 mM NaN₃, 0.5 mM CaCl₂, and 0.1 mM PMSF, and then separated by anion exchange chromatography. Our modified procedure uses different chromatographic steps for isolation of plasma gelsolin: a first chromatography on a DEAE-Sepharose 6B column (NaCl concentration gradient up to 0.1 M); a second chromatographic separation on a DE-52 column (with a buffer containing 10 mM Tris-HCl, pH 8.0, 0.1 mM EGTA, 1.5 mM NaN₃, and 0.1 mM PMSF) using a NaCl concentration gradient from 75 to 300 mM; and an optional third chromatography using 10 mM Tris-HCl, pH 8.0, containing 0.1 M NaCl, 0.1 mM EGTA, 1.5 mM NaN₃, and 0.1 mM PMSF on Sephacryl S-400. The assay used for column fractions was the test tube inversion assay (Pollard and Cooper, 1982). Samples from each elution tube (∼3 ml) were divided in aliquots, frozen in liquid nitrogen, and stored at −70°C.

Smooth muscle actin-binding protein (filamin) was purified from fresh chicken gizzard by the procedure of Feramisco and Burridge (1980). We modified the original method to eliminate variability from phosphocellulose chromatography, using only the fractions with highest purity obtained from DEAE-cellulose elution. Under these conditions, protein that is essentially homogeneous is obtained.

Aliquots of filamin were frozen in liquid nitrogen and subsequently stored at −70°C in a buffer containing 200 mM NaCl, 0.1 mM EDTA, 15 mM β-mercaptoethanol, and 20 mM Tris-acetate, pH 7.6 (Feramisco and Burridge, 1980). To avoid aggregates formed during freezing (Weihing, 1985), especially evident at low ionic strength (Davies et al., 1980), we centrifuged aliquots in an airfuge (Beckman Instruments, Inc., Palo Alto, CA; 10 min, 135,000 g). Thawed samples were used once and not refrozen. When high concentrations of filamin were needed (molar ratios F/A > 1:20), an overnight dialysis against depolymerizing G buffer containing 1 mM dithioerythritol was performed (excess of 100 vol); samples were centrifuged as described above and used within 8 h. This procedure avoids interference of high NaCl concentration, which may affect actin polymerization. We did not find any variability in results obtained for low filamin (and NaCl) concentrations of samples processed according to our protocol. However, we find a different behavior of high concentrations of filamin stored in high NaCl, which induces gelation and immobilization of actin.
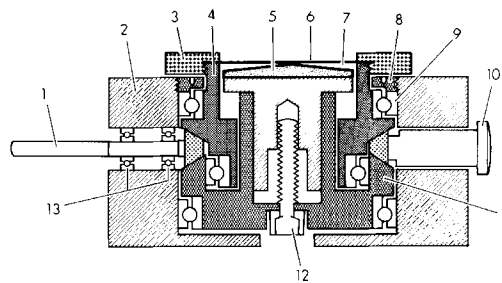


*Figure 1.* Schematic of the cone and plate rheometer described in the text (see Materials and Methods). Numbers in the drawing refer to (*1*) drive shaft (coupled to a motor); (*2*) rheometer external housing; (*3*) retaining ring, plate drive assembly; (*4*) cylindrical tube, plate drive assembly; (*5*) cone (cone angle, Θ = 1.5 degrees); (*6*) glass cover slip; (*7*) sample chamber; (*8*) retaining ring, bearing; (*9*) ball bearing, plate drive assembly; (*10*) brake with rubber cone that controls motion of cover slip relative to cone movement; (*11*) cylindrical tube, cone drive assembly; (*12*) cone positioner (screw that sets cone to cover slip distance); and (*13*) ball bearing, drive shaft assembly.

### Description of a Cone and Plate Rotational Rheometer

A rheoscopic device suitable for FPR-related techniques and image analysis has been constructed (Washington University Instrument Shop, St. Louis, MO). The rheometer (name used through this text) is a modification of an early Wells-Brookfield cone-plate viscometer adapted for light microscopy (Schmid-Schoenbein et al., 1969; Wells et al., 1961). The design of the instrument is shown in Fig. 1.

The rheometer is placed on the stage of a universal microscope (Zeiss, Oberkochen, Federal Republic of Germany), and connected to a variable speed drive. The drive system was designed to deliver controlled constant rotation over long periods of time, using a SSA 40-10-30 servo amplifier and a permanent magnet DC motor type U9M4T (PMI Motors, Syosset, NY). Experiments presented here cover a range of unidirectional shear rates of 0.04–12.66 s⁻¹, but the rheometer can cover a more extended range of 0.025–413.0 s⁻¹.

Shear rates were calculated using the expression (Martin et al., 1983):

$$\gamma = R/\psi,$$

where γ is the rate of shear (s⁻¹), R is the rotational velocity of the rheometer (in radians/s, and ψ is the rheometer angle between the cone and plate (in radians). This equation is valid only for cones with small angles. In our equipment the cone-plate angle is 1.5° (0.0262 radians). Although the actual shear rates are dependent on the geometry of the apparatus, they are independent of the distance from the cone tip.

The cone was machined from Plexiglas, and its transparency permits observation through the solution into the cone. This property was used to test solutions containing rhodamine-labeled actin for protein adsorption. Careful cleaning of the cone (three cycles of 2-propanol and water) and glass cover slips (five cycles of methanol and water) prevented protein adsorption to the cone and cover slip. Cover slips were discarded frequently and both pieces were air dusted before each use. We have not seen accumulation of fluorescence closer to the cover glass or the cone. Samples with actin concentrations >2 mg/ml may show adsorption to glass in our rheometer.

The relative distance of the cone tip with respect to the cover slip can be controlled with a screw in the base of the rheometer (see Fig. 1). The gap between them is observed illuminating through the microscope optics with an arc lamp and there is little movement of the tip position when observed under such conditions (i.e., the cone is symmetric). The temperature was measured with a thermistor (model 8040 A Multimeter; John Fluke Mfg Co., Inc., Everell, WA) and was always 21-23°C in experiments shown here.

Protein samples (containing actin with 10% rhodamine-labeled actin, gelsolin, and/or filamin) were prepared at room temperature in a 100-μl vol with or without the addition of Mg²⁺ (from MgSO₄) to start the polymerization. Aliquots of 75 μl were loaded onto the cone tip and a cover slip tightened into place with the retaining ring (see Fig. 1, element No. 3). Shearing of samples was then initiated and continued throughout polymer-

ization. Solutions were examined at ~0.65 cm from the rotation center, where the distance between the cover slip and the cone is ~170 µm. At the end of a measurement, the temperature was recorded as described above. Specific experimental detail about sample preparation is given in the legends for the respective figures.

## FPR and Microscopic Fluorescence Polarization Measurements

The FPR apparatus used is a modified version (Petersen et al., 1986) of the design of Koppel et al. (1976). All experiments (unless otherwise stated) were performed using a 16× microscope objective (Zeiss Ph 2, numerical aperture 0.35), which gives a Gaussian beam radius of $4 \times 10^{-4}$ cm measured by an image analysis method.

FPR experiments were carried out and analyzed as described by Tait and Frieden (1982b). The program used for analysis is based in a nonlinear curve-fitting procedure described by Bevington (1969), which uses a Marquandt algorithm applied to a variable number of terms in the series solution of diffusional fluorescence recovery after photobleaching (Axelrod et al., 1976). When microscopic fluorescence polarization was determined (see Figs. 5 and 6), the program was used to obtain average values of fluorescence and test possible photodamage of samples. A more detailed description of fitting procedures is given elsewhere (Petersen et al., 1986). For rhodamine-labeled actin the excitation wavelength of the argon-ion laser used was 515 nm.

The characteristic recovery time ($\tau_d$) of the fluorescence recovery is related to the apparent translational coefficient of the fluorophore, $D$, by the expression (Axelrod et al., 1976):

$$D = w^2/(4\ \tau_d),$$

where $w$ is the Gaussian beam radius.

In the experiments where microscopic fluorescence polarization was measured (Figs. 5 and 6), two polarizers were placed in the laser light path. The first polarizer, located immediately before the sample, ensured that a high degree of polarization was present in the incident light. Laser light is usually polarized in FPR experiments (a set of two polarizers regulated polarization before the first shutter), but some depolarization occurs in the optical path. The second polarizer was used in place of the normal barrier filter above the dichroic mirror in the universal microscope. This second polarizer is mounted in a holder that permits reorientation to measure both parallel and perpendicular orientations of the polarized light. Fluorescence reading was performed without photobleaching the samples, and apparent

steady-state fluorescence anisotropy can be calculated as in Lacowicz (1983).

## Results

### Actin Polymerization in the Absence of Shear

The incorporation of monomeric actin into polymer can be measured by an increase in rhodamine-labeled actin fluorescence on polymerization (Tait and Frieden, 1982b). The increase in fluorescence reaches ~50% when the polymerization is completed, and the extent of polymerization can be obtained from the fluorescence intensity before an FPR bleach is performed. The fluorescence intensity at a given time (i.e., $F_t$) is related to the initial fluorescence ($F_{t=0}$) and the final fluorescence ($F_\infty$) as an enhancement in fluorescence ($F_{(k)}$) (Axelrod et al., 1976) by the equation:

$$F_{(k)} = [F_{(t)} - F_{(t=0)}]/[F_{(\infty)} - F_{(t=0)}].$$

Fig. 2 shows experiments with 1 mg/ml actin containing 10% rhodamine-labeled actin in which the extent of polymerization (as measured by fluorescence enhancement, $F_{(k)}$) and the extent of immobility ($1 - X_m$, where $X_m$ is the mobile fraction) are plotted as a function of time after addition of 1 mM $Mg^{2+}$. These and all other experiments reported here were performed using the rheometer sample chamber and are the control experiments for those done in the presence of shear. The results obtained here are similar to those previously reported by Tait and Frieden (1982b) in that as polymerization proceeds, the actin becomes immobilized until it is essentially totally immobile. Under the conditions used here, the immobilization and extent of polymerization occur approximately in parallel. It is also possible to measure the apparent diffusion coefficient as a function of time in these experiments. We find as expected, that the
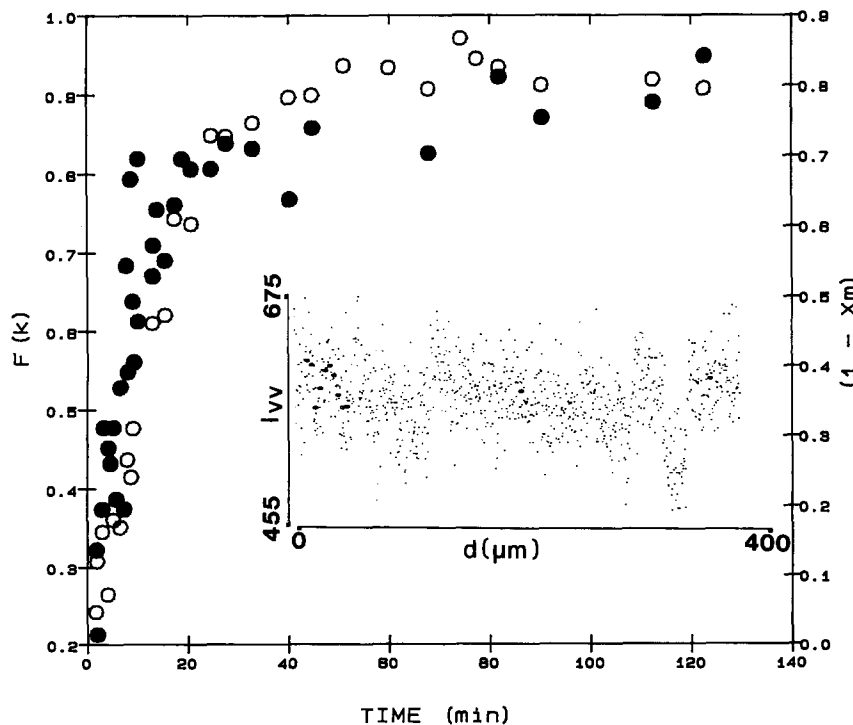


*Figure 2.* Time course of actin polymerization followed by FPR. Measurements of normalized fluorescence enhancement ($F_{(k)}$ = $F_{(t)} - F_{(t=0)}$ /$F_{(\infty)} - F_{(t=0)}$, *solid circles*) and of the fraction of actin immobilized ($1 - X_m$, *open circles*) are represented as a function of time after addition of 1 mM $Mg^{2+}$ to a 1 mg/ml actin solution (10% rhodamine-labeled actin). Experiments were performed without shear at 22°C in depolymerizing buffer (0.2 mM $CaCl_2$, 0.2 mM $Na_2ATP$, 1.5 mM $NaN_3$, and Tris-HCl, pH 8.0) in the rheometer sample chamber. *Inset,* a fluorescence scan of the rheometer surface after actin polymerization is complete. $I_{VV}$ is the fluorescence intensity of samples observed through parallel polarizers (arbitrary units are recorded counts per channel). The abscissa represents the distance $d$ (in µm) that the rheometer was moved during the experiment. In all the experiments the beam size radius was $4 \times 10^{-4}$ cm (see Materials and Methods).

diffusion of actin becomes slower as the polymerization proceeds until no diffusion is apparent (Tait and Frieden, 1982b). We believe that the state in which actin filaments are unable to diffuse is equivalent to forming a filamentous actin gel. After polymerization is complete, it is possible to scan the filamentous actin solution by moving the rheometer in the beam of the laser at low intensity. Fig. 2 (inset) shows that the solution appears fluorescently homogeneous.

## Actin Polymerization in the Presence of Shear

Experiments were performed as above except that after $Mg^{2+}$ was added to the nonfilamentous actin and the solution placed in the rheometer, it was subjected to a known

shear. In this case it was necessary to stop the shear for the measurement of diffusion coefficients and mobility ($X_m$). Since the polymerization occurs over a long time period and the measurements take $\sim$40 s, it was important to show that stopping the shear did not affect the results. This was demonstrated in experiments in which only a few measurements were made over time and compared to experiments in which many measurements were performed. The results were the same in both cases for shear rates used in this paper. It is of interest that the rate of polymerization did not change over the range of shear rates applied (0.05–12.66 s$^{-1}$), indicating that there was no breakage of actin filaments under these conditions.

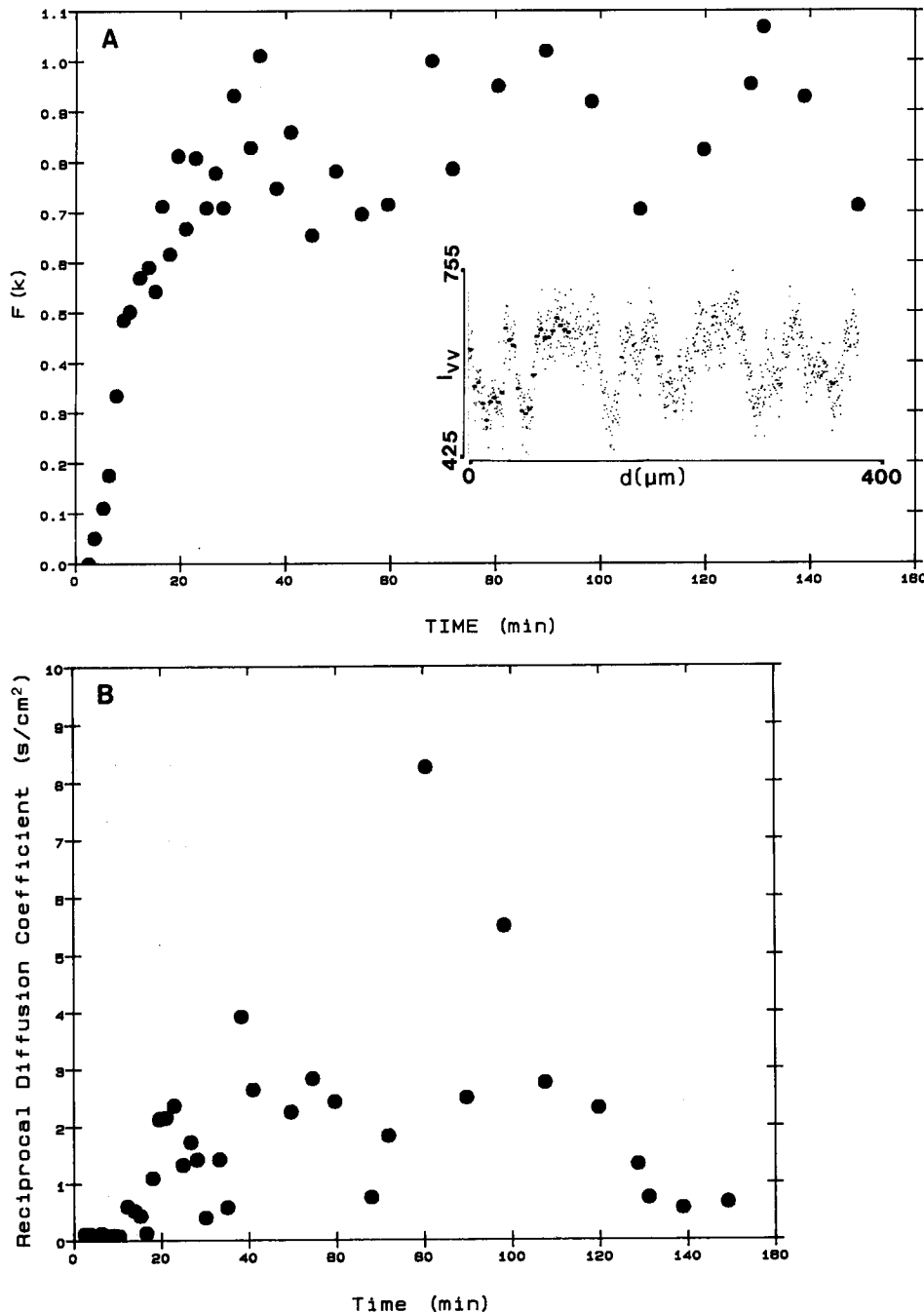Fig. 3 shows the results of these experiments with respect



Figure 3. (A) Time course of normalized fluorescence enhancement (F[k]) for actin polymerized under shearing conditions (one rheometer turn per 100 min; i.e., a shear rate (γ) of 0.04 s$^{-1}$). At each point on the graph, the rheometer was stopped and the fluorescence measured. The FPR experiment was performed as described in Materials and Methods. Experimental conditions as in Fig. 2 except that polymerization was induced with 2 mM $Mg^{2+}$. Inset, a fluorescence scan of the rheometer surface after actin polymerization under shear is complete. As in Fig. 2, the ordinate shows arbitrary units for fluorescence polarization (I$_{VV}$) and the abscissa represents movement of the rheometer (distance $d$) in μm. (B) Plot of reciprocal diffusion coefficients of actin polymerizing under shear measured using the same conditions as in A. The mobile fraction ($X_m$) also shows an irregular distribution (data not shown).

1480

to the fluorescence enhancement (*A*) and diffusion coefficients (*B*). At early stages on polymerization, the diffusion coefficient decreases as expected. However, as the polymerization approaches completion, the fluorescence intensity and diffusional properties measured by FPR become quite variable. Since measurements are made in different portions of the solution, it seemed likely that the variation represented nonuniformity of the sample. Indeed, when the solution is scanned using incident light, large and discrete fluctuations in fluorescence are observed (Fig. 3 *A*, *inset*). Similar results were seen at all the shear rates applied. This inhomogeneity remained after stopping the shear up to 2 h. Thus, not only is some structure of filamentous actin induced by shearing but it also appeared to be stable. We have not yet measured the dissipation of the microheterogeneity induced by shear.

To further explore the observed inhomogeneity, we used actin filaments with different length distributions. As shown previously (Harris and Schwartz, 1981; Doi and Frieden, 1984; Janmey et al., 1986), the presence of plasma gelsolin (brevin) will act to narrow the length distribution of actin filament at certain G/A ratios. At G/A ratios of 1:50 or 1:100, there is probably a rather narrow range of lengths while at a G/A ratio of 1:300 or less, the distribution is wider. Under either of these conditions, actin is not totally immobilized so it is possible to obtain diffusion coefficients as a function of time or applied shear.

Fig. 4 shows that at G/A ratios of 1:100 and 1:300, there is a decrease in the diffusion coefficient of the sheared sample relative to that of the unsheared sample. The decrease in the diffusion coefficient is dependent on the total amount of shear applied since the results were identical for shear rates of 0.05–1.29 s$^{-1}$. The decrease in diffusion coefficient is more apparent for larger filament lengths (G/A ratio of 1:300; Fig. 4, *closed circles*) than for the shorter filaments (G/A ratio of 1:100; Fig. 4, *open circles*), and there is no apparent change for very short filaments (G/A 1:50; data not shown). As will be discussed later, we believe that this behavior is a consequence of bundling of filaments (i.e., lengthwise filament–filament interactions), induced by shearing the sample. Shear rates and the time period under which G/A mixtures were polymerized (0.5–1.0 h) ensure that the polymerization was complete (not shown). The mobility of actin–gelsolin filaments (measured by FPR) did not change when they were subjected to shear (see legend to Fig. 4).

## Fluorescence Polarization Changes after Stopping Shear

The design of the rheometer precluded measuring changes in birefringence and so we examined changes in fluorescence polarization as an indicator of filament orientation. When 1 mg/ml actin (10% rhodamine-labeled actin) is allowed to polymerize under shearing conditions and the rheometer is stopped, the fluorescence polarization changes as a function of time. This fluorescence relaxation is quite variable. Fig. 5 shows experiments in which actin gels are observed after removing the linear shear stress with the polarizing and analyzing polarizers in parallel (light intensity is then $I_{vv}$). In the sample subjected to shear, there is a slow and sometimes complex decay of the fluorescence after stopping the rheometer (dwell times of 400 ms were used in our counting device, which cover 7 min per individual experiment as shown in Fig. 5, *A*, *B*, and *C*). In a similar experiment this slow decay was not observed in the absence of polarizers. Thus, the decay of $I_{vv}$ observed probably reflects some slow change in the anisotropic behavior of the actin gels (cf. Figs. 3 and 5), but the microheterogeneity obtained is stable
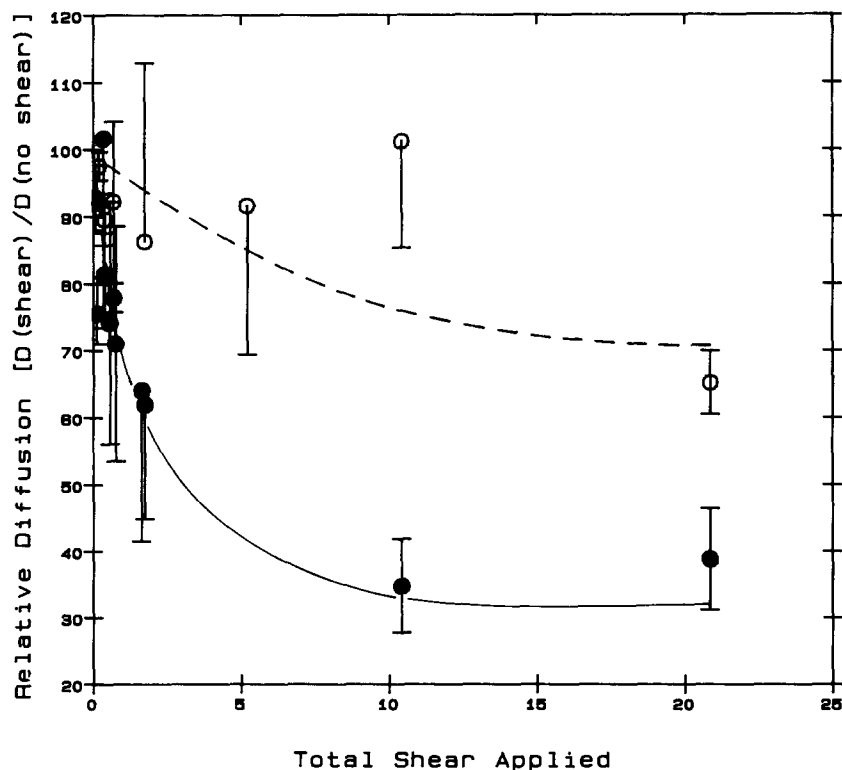


*Figure 4.* Effect of shear on the diffusion coefficient of actin polymerized in the presence of gelsolin (G/A molar ratios 1:100 and 1:300). Relative diffusion coefficients [D(shear)/D(no shear)] were determined by FPR: D(shear) is the diffusion coefficient measured after samples were sheared at various shear rates and D(no shear) is the value for an unsheared sample. Average values (at least five individual measurements in a 30-min period after stopping shear) are used in calculating this ratio. There is no change in the prebleach fluorescence level or the mobile fraction of fluorophores ($X_m$) by shear, only an increase in recovery times ($\tau_d$), indicative of larger average polymers. Experiments are shown for G/A filaments with a G/A ratio 1:300 (*solid circles*) and G/A ratio 1:100 (*open circles*). Mobility estimated by FPR is similar for sheared and unsheared samples (70–75% for G/A 1:300 filaments and 90–95% for G/A 1:100 filaments; see Doi and Frieden, 1984). The change in the diffusion coefficient is independent of the shear rate (ranging from 0.05 to 12.66 s$^{-1}$), but dependent on total shear applied. An estimate of the strain for these experiments (shear is applied on samples that undergo polymerization and it is not a linear function) ranges from 4 to 170%.
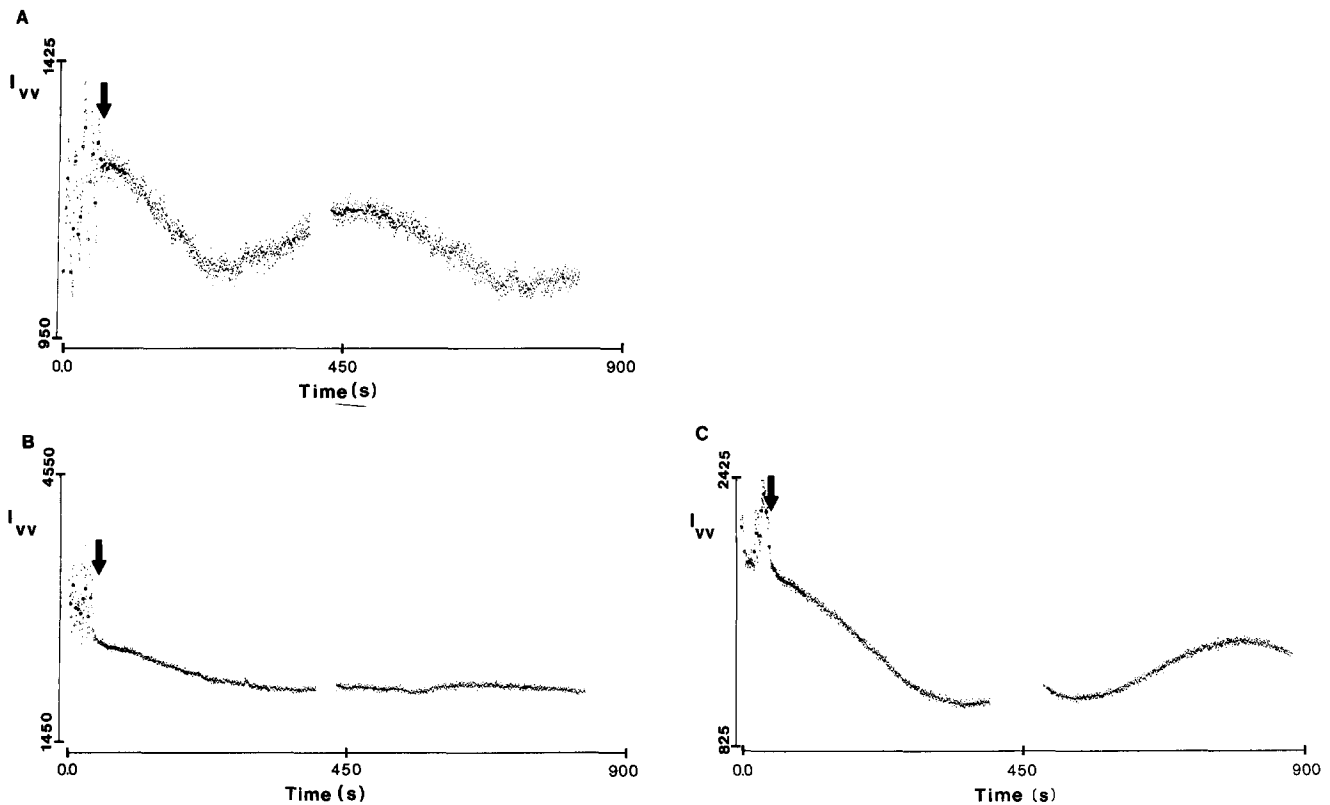
Y-axis: Relative Diffusion [D (shear) /D (no shear)]

X-axis: Total Shear Applied

*Figure 5.* Changes in fluorescence polarization (using parallel polarizing and analyzing polarizers, $I_{VV}$) after stopping shear of actin polymerized under shear. Actin (1 mg/ml, 10% rhodamine-labeled actin) was polymerized under shear by addition of 1 mM $Mg^{2+}$. After 1 h of shear (rate of shear = $0.58\ s^{-1}$), the rheometer was stopped and polarized fluorescence ($I_{VV}$) was followed for several minutes. *A, B,* and *C* are data from different spots and are representative of the relaxation processes observed in the sample. The first experiment of each includes 100 channels of recording before shear is eliminated (*arrow point*), and a second set of data ($\sim$450 s later) are included to show the continuity of the relaxation process. Various shear rates ranging from 0.06 to 12.66 $s^{-1}$ gave overall effects (complex relaxation and also oscillatory behavior) comparable to the ones shown in this figure.

in the time range used in these experiments (up to 30 min). In experiments without shear there is no change in the fluorescence intensity, indicating no inhomogeneity and no photobleaching of the filaments under the incident light beam (not shown).

As in the experiments described earlier, we wished to examine the fluorescence polarization properties of filaments of different length distributions as adjusted by the presence of gelsolin. Fig. 6 shows results observed for several G/A ratios sheared for 1 h (shear rate of 1.29 $s^{-1}$; shear rates in the range 0.05–1.29 $s^{-1}$ give similar results). At this time, when polymerization was complete, the rheometer was stopped and the changes in fluorescence polarization recorded. The data show that there is a transition between no relaxation behavior (G/A ratio 1:50; Fig. 6 *A*), to a detectable decay (G/A ratio 1:100; Fig. 6 *B*), to complex behavior where rather different patterns of relaxation are observed at different positions (G/A ratio 1:300; Fig. 6, *C* and *D* ). In addition, the experiment in Fig. 6 *A* (G/A ratio 1:50) shows that there is no photobleaching of the filaments at the laser intensity used.

## The Effect of Filamin on Actin Filaments Formed in the Presence of Gelsolin

Filamin decreases diffusion coefficients obtained from G/A filaments formed in the absence of shear. The ratio of the

diffusion coefficient measured in the presence of filamin (D[filamin]) to that in the absence of filamin (D[0]) for different F/A molar ratios (ranging from 1:600 to 1:9) is shown in Fig. 7. This effect is again proportional to the average length of filaments in the range of G/A ratios of 1:300 to 1:50. At F/A ratios higher than 1:20, filamin induces association of actin filaments (and probably gelsolin–actin filaments) into bundles (Weihing, 1985). Concentrations of filamin as low as a F/A ratio of 1:300 have apparent effects in diffusional parameters. We observed changes in steady-state fluorescence anisotropy at F/A ratios of 1:600, whether it is measured in the rheometer chamber or in a spectrofluorometer cuvette (not shown).

The change in diffusion is proportional to the amount of filamin and to the average filament length. Assuming a saturation type behavior for the effect of filamin upon diffusion coefficients, values for the number of moles of filamin bound per actin polymer that give 50% maximal effect in diffusion coefficients were obtained by a nonlinear regression program (Duggleby, 1981). The efficiency is very similar for filaments of different length, values are 10.2 (G/A ratio 1:300) and 13.4 (G/A ratio 1:100) mol of filamin bound per mol of gelsolin–actin filament (i.e., a ratio of $\sim$10 filamin molecules per filament); data from gelsolin–actin filaments at G/A ratio 1:50 are not fitted adequately by the program algorithm. It should be noted that these values represent the effect of
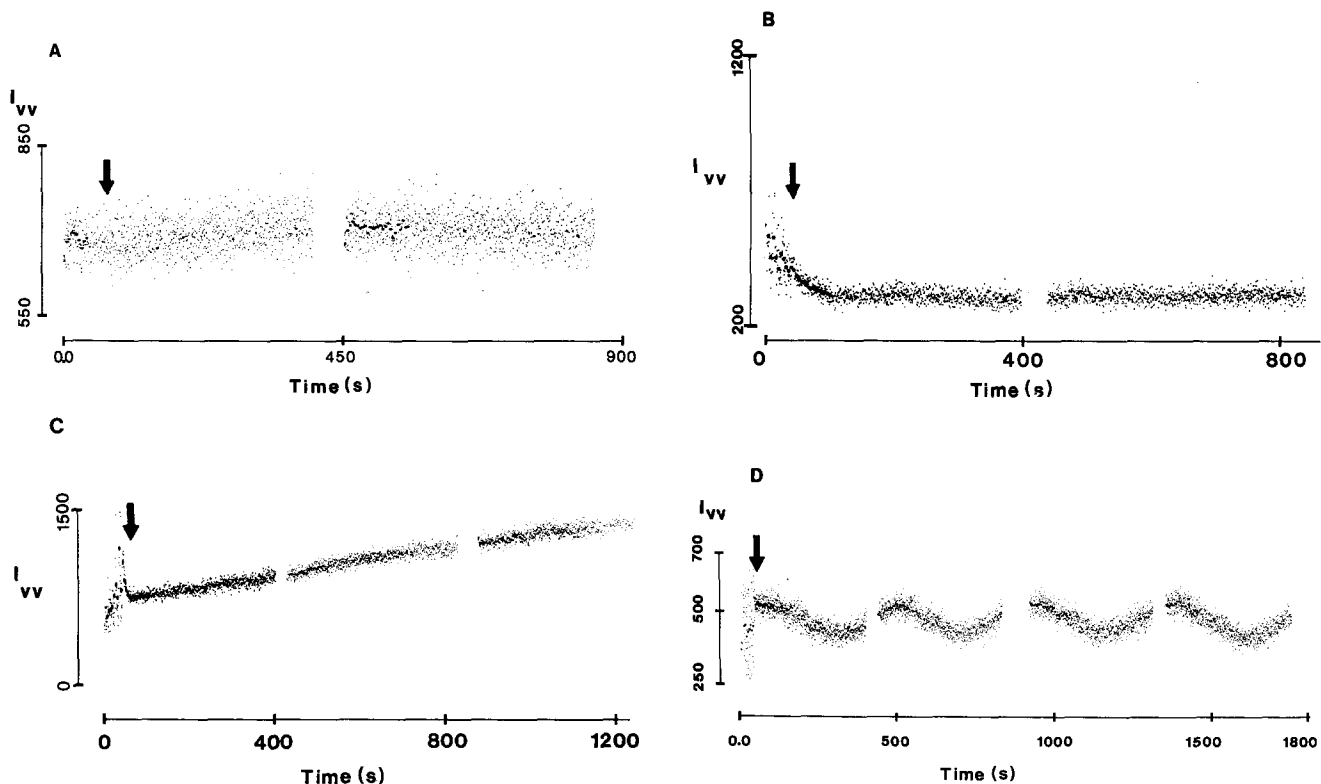
*Figure 6.* Effect of gelsolin on changes in fluorescence polarization ($I_{VV}$) of polymerized actin after stopping shear. Gelsolin was added to control the length of the average filament formed. Actin–gelsolin mixtures (0.5 mg/ml actin, 10% rhodamine-labeled actin) with G/A molar ratios from 1:50 to 1:300 were polymerized under shear (rate of shear of 1.29 s$^{-1}$) by addition of 2 mM Mg$^{2+}$. Samples were prepared as indicated in Fig. 2 and subsequently placed in the rheometer chamber. After 1 h, the rheometer was stopped followed by polarized fluorescence ($I_{VV}$), as in Fig. 5, performing several consecutive experiments (which are shown as data sets in these figures). Molar ratios of gelsolin to actin are (*A*) 1:50, (*B*) 1:100, and (*C* and *D*) 1:300; the decrease in fluorescence after stopping the shear (relaxation) and the microheterogeneity appeared at a G/A molar ratio of ~1:100. This behavior can also depend on the relative orientation of the shear field to the polarizers (see text).
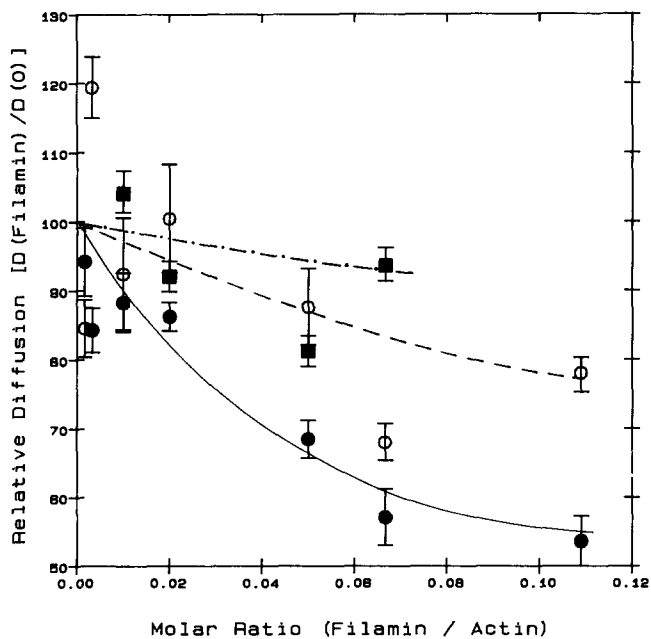


*Figure 7.* Effect of chicken gizzard filamin on diffusional properties of gelsolin–actin mixtures polymerized in the absence of shear. Relative diffusion coefficients (D[filamin]/D[0], where D[filamin] is the diffusion coefficient of mixtures polymerized in the presence of

filamin in diffusion of gelsolin–actin filaments, they may not correlate with filamin binding to individual actin molecules. The maximal effect in diffusion (minimal value of the ratio D[filamin]/D[0] obtained) were 0.21 (G/A ratio 1:300) and 0.02 (G/A ratio 1:100).

## Discussion

In this study, we have demonstrated that controlled shear of polymerized actin generates spatial heterogeneity of the filament solution and large fluctuations in the diffusion coefficients and mobility determined by FPR (cf. Figs. 2 and 3). In addition, fluorescence polarization experiments that qualitatively measure the relaxation of the filament distribution after cessation of the shear yield complex and variable patterns of change (Figs. 5 and 6). Experiments with gelsolin-capped filaments of defined length demonstrate that the

filamin, and D[0] is the diffusion coefficient of a mixture polymerized in the absence of filamin) were determined by FPR for gelsolin–actin mixtures containing 0.5 mg/ml total actin concentration (10% rhodamine-labeled actin), made at G/A ratios of 1:50 (— · —, ■), 1:100 (— —,○), and 1:300 (—,●) by polymerizing with 2 mM Mg$^{2+}$ in the presence of various concentrations of filamin (F/A ratios 1:600 to 1:9).

magnitude of the shear-induced change in diffusion is length dependent (Fig. 4). The presence of filamin during polymerization without shear induced a similar change in diffusion coefficients (Fig. 7) in a range of concentrations where it bundles actin (Weihing, 1985).

The spatial fluctuations in fluorescence intensity are certainly due to fluctuations in filament density (i.e., actin concentration), since shear should not affect the basic spectroscopic properties of the fluorophores. It is most likely that regions of high filament concentration result from lateral aggregation of the filaments. This would account for the decrease in diffusion coefficients of gelsolin–actin filaments formed under shear (Fig. 4) and for the complex effects on fluorescence polarization (Figs. 5 and 6). Shear would enhance the lateral aggregation by aligning the filaments to an extent where molecular contacts are established and propagated cooperatively along them (DeRosier and Tilney, 1982).

The magnitude of the shear-induced heterogeneity of filament density and diffusion increase with increasing filament length. The observation that the decrease in the diffusion coefficients of the gelsolin–actin filaments formed under shear varies with the total amount of shear (measured as the total number of rheometer rotations) rather than the rate of shear (rotational velocity of the rheometer) suggests that the formation of aligned aggregates (and the microheterogeneity observed) is a cumulative process. The lack of dependence on shear rate (in the range 0.05–12.66 s$^{-1}$) suggests also that the extent of alignment produced at the lower rates was already sufficient to aggregate the filaments into bundle-like structures. Hence it seems likely that the presence of shear over long periods during polymerization promotes the formation of linear aggregates. The growing bundle presents an interface to grow new filaments associated to itself (acting as a "primer"). The cumulative nature of this process implies strong molecular interactions between actin filaments formed under shear, and a very stable bundle structure. Models for diffusion of rod-like macromolecules that consider important only steric hindrance (Jain and Cohen, 1981) will predict a more transient phenomenon.

It is surprising that shear did not appear to fragment filaments. This may result from the relatively low shear rates used, but the results clearly indicate that rather than breaking, the filaments align into bundles. We have not yet examined whether much higher shear would break filaments (i.e., 200–1,000 s$^{-1}$; Jen et al., 1982). At G/A ratios <1:100, shear alone cannot generate microheterogeneity in actin gels (not shown; see Fig. 6 A), but induces microheterogeneity in longer filaments. This would suggest that a critical length is needed to start protein–protein interaction, and is discussed below in terms of models for polymer dynamics.

Measurements of polarization of actin fluorescence can provide an indicator of the extent of alignment of the actin filaments. The large steady-state anisotropy (r) of rhodamine-actin fluorescence (r is in the range 0.250–0.275 for our experimental conditions) indicates that the fluorophore is rigidly fixed on the actin monomer (Lacowicz, 1983). We further suppose that the rhodamine molecule retains a defined orientation relative to the actin monomer itself. Therefore the fluorescence from rhodamine molecules on an actin filament will be polarized in a fixed direction relative to the filament axis, and the observation of regions of higher

and lower intensity of polarized fluorescence in a sample that has been subjected to shear suggests that there are regions with greater and lesser extents of aligned filament aggregation. As measured by fluorescence, the width of these aggregates is in the order of thousands of microns.

We have performed microscopic fluorescence polarization experiments (Figs. 5 and 6) to ascertain if the microheterogeneity generated under shear could relax after instantaneous elimination of the shear field. Dissipation of the microheterogeneity will imply a recovery of a homogeneous fluorescence across the sample (isotropy). We have not yet observed this for up to 16 h (Cortese and Frieden, unpublished results). However, the relaxation observed in experiments of Figs. 5 and 6 occurs during the first 30 min after we eliminated the linear shear. The behavior observed is complex, but some characteristics of these experiments can be described. First, actin samples look heterogeneous under polarized light, although homogeneous when observed without polarizers. That indicates that alignment plays a role in the effect of shear. When the fluorescence polarization of a single spot is followed after stopping the rheometer, there is relaxation to a less organized state (i.e., to lower values of I$_{VV}$). For actin, this process is completed in ∼150–300 s.

Second, the actual position of the laser beam is a critical issue. The rheometer used applies shear in a direction perpendicular to its radius, and if there is appreciable orientation of the filaments formed under a shear field, it should be parallel to the shear forces. When the changes of polarized light with time are measured, the polarizers can have different relative orientations with respect to the shear field. Thus the actual change (relaxation) in fluorescence may depend on the orientation of the filaments relative to the polarized light. Changes shown in Figs. 5 and 6 may be attributed to slow rotation and redistribution processes between filaments perpendicular and parallel to the polarizers. The oscillatory behavior (Fig. 5, B, C, and D) and the fact that some relaxation actually occurs in the direction of an increase in fluorescence (Fig. 6 C) could support this hypothesis.

Third, the actual relaxation process may involve more than one component. In fact, Fig. 4 B shows an oscillatory process that slowly goes to low values of fluorescence, which may imply an extremely slow redistribution of filaments to areas with low concentration of them, tending to a more homogeneous final state. This would indicate a continuous recovery of microheterogeneity after elimination of shear (and stress), but experiments shown here do not have enough sensitivity to estimate that time. In some experiments, a fast first relaxation was found (∼4–8 s; Fig. 5 B), possibly related with local realignment of filaments previously separated in the shear field or randomization of free filaments. All these experiments show that the final fluorescence (and extent of decay) depends on the area observed, and they indicate that free filaments may rotate.

The complex behavior of the microheterogeneity obtained by polymerizing actin under shear implies processes of interfilament association that are usually ignored in polymer dynamics. There are three regions that should be considered in discussing the behavior of linear polymers in solution. In the dilute regime polymers move independently, while in the semidilute solutions polymer domains overlap and interact. At concentrations within the semidilute regime there is a significant change in rotational diffusion coefficients (Doi

and Edwards, 1986). An approximate calculation for gelso-lin–actin filaments made at G/A ratios of 1:100 shows that they are approximately in the region between dilute and semidilute regimes.[2] A transition in properties for un-sheared filaments >1:100-G/A ratio was observed by quasi-elastic light scattering (Janmey et al., 1986), and attributed to restricted diffusional motion of the polymer molecules. We have observed similar differences for sheared samples of gelsolin–actin filaments (Fig. 5).

A model of viscoelastic properties would be useful to un-derstand actin rheology in physical terms. However, there has been some disagreement in the literature about which theoretical model is the simplest for simulating in vitro me-chanical properties of cytoskeletal proteins. It is well known that actin exhibits macroscopically positive thixotropy (Kasai et al., 1960; Maruyama et al., 1974; Zaner and Stos-sel, 1983), and that it resists brief mechanical insult but de-forms slowly under external forces (Petersen et al., 1982; Zaner and Stossel, 1983; Sato et al., 1984, 1987). Two different major classes of models have been proposed to ex-plain the rheological behavior of actin at the microscopic level. In the first class are noninteractive models, which ig-nore polymer–polymer (i.e., actin–actin) interactions as a component of hydrodynamic behavior. Filaments are visual-ized as stiff rods only restricted by topological constraints (Zaner and Stossel, 1982; 1983; Zaner, 1986; Doi and Ed-wards, 1986). This model is based on Doi and Edwards (1978) theory for polymer motion in concentrated solutions, extended for rod-like macromolecules by Jain and Cohen (1981; for a review on these ideas see de Gennes and Leger, 1982).

A second class of models attempts to explain rheological properties of actin by filament–filament interaction, from fixed cross-links ("rubber"like theories; Aklonis and Mac-Knight, 1983) to more or less reversible attachment between filaments. The actin gel is considered to be a network of fila-ments bound by reversible interactions, which would behave as a viscoelastic solid (Ferry, 1980). This point of view in-volves filament–filament binding over other modes for re-stricting diffusion. Since filamentous actin is immobilized by such interactions (Tait and Frieden, 1982a; Doi and Frieden, 1984; Sato et al., 1985), the dynamic behavior of these bonds and their relationship with actin-binding proteins (Sato et al., 1987) could be enough to explain rheological properties of actin gels.

It is unfortunate that neither model accounts for the contri-bution of bundling to the mechanical properties of actin, and our results show that such phenomenon (interfilament as-sociation) may represent an important factor in actin rheol-ogy as it is related to cell function. We believe that the cur-rently used models of diffusion for rigid rods (Doi and Edwards, 1978, 1986; Jain and Cohen, 1981) should be

modified to include reversible association (with or without cooperativity) between polymers so as to explain completely actin rheology.

A solution of rod-like particles of sufficient length or con-centration can spontaneously form an ordered liquid phase (Onsager, 1949; Flory, 1956; Doi and Edwards, 1986). This process is preferential for the longer particles (Lekkerkerker et al., 1984) and occurs for concentrations higher than $5/cL^2$; see Footnote 2). Those concentrations are only 2–8 times higher than actin concentrations used in our experi-ments. For actin (assuming a length of 1,000 monomers long on average), an increase of only 2.35 times in concentration in a particular area can drive the polymers above the concen-tration at which the polymer mixture becomes a liquid crys-tal. It is very likely that shear, through an alignment of grow-ing filaments parallel to the shear field, may cause local increases in concentration, which consequently serve as points of crystal nucleation. The possible organization of ac-tin filaments into liquid crystals has been discussed in the literature (Kasai et al., 1960; Buxbaum et al., 1987; Ito et al., 1987). The solutions of actin filaments that we have stud-ied do not display apparent phase separation, although a microphase separation could explain the microheterogeneity (Cortese, J. D., and C. Frieden, unpublished results).

We have supposed here that the formation of the aligned aggregates that are detected in our measurements could re-quire many weak interactions among the filaments, and that the formation of the aligned aggregates could result from a cooperative process initiated by the shear-dependent forma-tion of a nucleus of aligned filaments. Thus, long filaments would bind better along their length than short filaments. This model is consistent with the observation on gelso-lin–actin filaments that the aligned aggregates formed more readily from longer filaments (cf. Fig. 4). It has been reported that nonfilamentous actin polymerizes under shear (Borejdo et al., 1981), and that nonfilamentous actin and some actin-binding proteins have properties of a viscoelastic solid (Sato et al., 1985, 1986). A transient interaction be-tween molecular binding sites could explain such otherwise surprising behavior, and it indicates that actin may have a strong sensitivity to shear. We visualize the association pro-cess as similar to the crystallization of soluble proteins (Oosawa and Asakura, 1975).

The use of a bundling protein from chicken gizzard (fila-min; for a review see Weihing, 1985) during polymerization of gelsolin–actin filaments in the absence of shear (Fig. 7) shows that at concentrations where filamin induces bundling (bundles are visible at the level of optical microscopy and by polarization in a range of F/A molar ratios 1:50 to 1:10) there is a decrease in translational diffusion coefficients similar to what is induced by shear. In this range of concentrations, filamin aligns filaments and increases fluorescence aniso-tropy; even a F/A molar ratio as low as 1:600 modified fluorescence anisotropy from gelsolin–actin filaments (Cor-tese, J. D., and C. Frieden, unpublished results). A compari-son between FPR data used in Figs. 4 and 7 indicates that the main effect is exerted (either by shear or by filamin addi-tion) in the recovery times (not shown). There is no destruc-tion of filaments by shear (the mobile fraction $X_m$ should in-crease if that is the case) or a decrese of the mobile fraction by filamin addition. This suggests that the average length dis-tribution of actin filaments increases during shear or by

2. Polymer solutions are considered dilute if $c < 1/L^3$ (where $c$ is the poly-mer number concentration and $L$ is the polymer length). The semidilute re-gime occurs when $1/L^3 < c < 1/d \cdot L^2$ (where $d$ is the polymer diameter, as-suming a rod-like particle). If $c \cdot L^3 > 1$, the solution is in the lower limit of the semidilute regime (Doi and Edwards, 1986). Approximate values of $cL^3$ for gelsolin–actin filaments made at molar ratios (G/A) of 1:300, 1:100, and 1:50 are 150, 1.61, and 0.38, respectively (actin concentration 0.5 mg/ml, and assuming 28.2 Å as actin monomer length; Hanson and Lowy, 1963). For gelsolin–actin filaments made at a ratio 1:100 and 1:50, this con-centration is in the lower limit of the semidilute regime.

filamin addition and strongly supports a bundling model for aggregation in the presence of shear or actin-binding proteins as filamin. Reannealing seems an unlikely explanation: it will not explain the dependence of the total shear rate for shear effects, and it will not be a preferential process for filamin-actin bundling (end-to-end vs. side-to-side contacts between filaments). In addition, FPR experiments performed over long periods of time after shear was eliminated give similar diffusion coefficients (recorded up to 1 h, data not shown). However, length redistribution and complete disappearance of microheterogeneity may still occur in extremely long times.

The destruction of the actin network and subsequent realignment along the shear field of newly formed filaments could facilitate the bundling otherwise absent. This kind of situation may be important for cytoskeleton dynamics, and in fact destruction and creation (turnover) of actin networks under shear could be regarded as a factor in the dynamics of cellular structures as stress fibers. It has been shown that stress fibers can be created in vitro by applying linear shear fields to human vascular endothelial cells (Franke et al., 1984), and this induced alignment could be reflecting the microscopic effects described in this paper for actin filaments. In vivo, tension applied over cells may induce a fast microscopic heterogeneity, being a primer for later organization of fibers (Taylor et al., 1973; Singer and Pudney, 1984; Joshi et al., 1985). Actin-binding proteins may then regulate the stability of the newly formed fibers.

Little is known about the interplay of actin and actin-binding proteins in the presence of mechanical forces. It has been assumed that actin develops a gel structure that is more or less homogeneous (isotropic) in the three directions of space (even in the presence of several actin-binding proteins; see Stossel, 1986). Experiments presented here indicate a different situation (at least in the presence of shear and some actin-binding proteins), with an anisotropic gel structure that could represent one of many transient states of the rheological behavior of actin. Both extremes should be considered in a complete picture of actin rheology. Then, there might be two limiting states in an actin gel: (*a*) a "resting" gel, which is more homogeneous and perhaps could be modelled using reptational theories (Stossel, 1986); and (*b*) an "active" actin gel, with portions organized into an anisotropic structure (partially a viscoelastic solid and a viscoelastic liquid) under exposure to biochemical agents as actin-binding proteins or mechanical forces (shear). Some of the properties ("activities") of these gels are possibly important in the generation of a spatial anisotropy in the living cytoplasm (Sato et al., 1983, 1984) and in the dynamics of actin-containing structures as stress fibers.

## References

Aklonis, J. J., and W. J. MacKnight. 1983. Rubber elasticity. *In* Introduction to Polymer Viscoelasticity. 2nd ed. John Wiley & Sons Inc., New York. 102–138.

Axelrod, D., D. E. Koppel, J. Schlesinger, E. L. Elson, and W. W. Webb. 1976. Mobility measurement by analysis of fluorescence photobleaching recovery kinetics. *Biophys. J.* 16:1055–1069.

Bevington, P. R. 1969. Data Reduction and Analysis for the Physical Sciences. McGraw-Hill Inc., New York. 336 pp.

Borejdo, I., A. Muhlrad, S. J. Leibovich, and A. Oplatka. 1981. Polymerization of G-actin by hydrodynamic shear stresses. *Biochim. Biophys. Acta.* 667:118–131.

Bradford, M. M. 1976. A rapid and sensitive method for the quantitation of microgram quantities of protein utilizing the principle of protein-dye binding. *Anal. Biochem.* 72:248–254.

Buxbaum, R. E., T. Dennerll, S. Weiss, and S. R. Heinemann. 1987. F-actin and microtubules suspensions as indeterminate fluids. *Science (Wash. DC).* 235:1511–1514.

Chaponnier, C., P. Patebex, and G. Gabbiani. 1985. Human plasma actin-depolymerizing factor. Purification, biological activity and localization in leukocytes and platelets. *Eur. J. Biochem.* 146:267–276.

Cooper, J. A., J. Bryan, B. Schwab III, C. Frieden, D. J. Loftus, and E. L. Elson. 1987. Microinjection of gelsolin into living cells. *J. Cell Biol.* 104: 491–501.

Davies, P. J. A., D. Wallach, M. Willingham, I. Pastan, and M. S. Lewis. 1980. Self-association of chicken gizzard filamin and heavy merofilamin. *Biochemistry.* 19:1366–1372.

de Gennes, P. G., and L. Leger. 1982. Dynamics of entangled polymer chains. *Annu. Rev. Phys. Chem.* 33:49–61.

DeRosier, D. J., and L. G. Tilney. 1982. How actin filaments pack into bundles. *Cold Spring Harbor Symp. Quant. Biol.* 44:525–540.

Doi, M., and S. F. Edwards. 1978. Dynamics of rod-like macromolecules in concentrated solution. Part 1. *J. Chem. Soc. Faraday Trans.* II. 74:560–570.

Doi, M., and S. F. Edwards. 1986. The Theory of Polymer Dynamics. Clarendon Press, Oxford. 391 pp.

Doi, Y., and C. Frieden. 1984. Actin polymerization. The effect of brevin on filament size and rate of polymerization. *J. Biol. Chem.* 259:11868–11875.

Duggleby, R. G. 1981. A nonlinear regression program for small computers. *Anal. Biochem.* 110:9–18.

Elson, E. L. 1988. Cellular mechanics as an indicator of cytoskeletal structure and function. *Annu. Rev. Biophys. Biophys. Chem.* 17:397–430.

Feramisco, J. R., and K. Burridge. 1980. A rapid purification of α-actinin, filamin, and a 130,000-dalton protein from smooth muscle. *J. Biol. Chem.* 255:1194–1199.

Ferry, J. D. 1980. Viscoelastic Properties of Polymers. 3rd ed. John Wiley & Sons Inc., New York. 55 pp.

Flory, P. J. 1956. Phase equilibria in solutions of rod-like particles. *Proc. R. Soc. Lond. A* 234:73–89.

Franke, R.-P., M. Grafe, H. Schnittler, D. Seffge, C. Mittermayer, and D. Drenckhahn. 1984. Induction of human vascular endothelial stress fibres by fluid shear stress. *Nature (Lond.).* 307:648–649.

Hanson, J., and J. Lowy. 1963. The structure of F-actin and of actin filaments isolated from muscle. *J. Mol. Biol.* 6:46–60.

Harris, D. A., and J. H. Schwartz. 1981. Characterization of brevin, a serum protein that shortens actin filaments. *Proc. Natl. Acad. Sci. USA.* 78:6798–6802.

Houk, T. W., Jr., and K. Ue. 1974. The measurement of actin concentration in solution: a comparison of methods. *Anal. Biochem.* 62:66–74.

Ito, T., K. S. Zaner, and T. P. Stossel. 1987. Nonideality of volume flows and phase transitions of F-actin solutions in response to osmotic stress. *Biophys. J.* 51:745–753.

Jain, S., and C. Cohen. 1981. Rheology of rodlike macromolecules in semidilute solutions. *Macromolecules.* 14:759–765.

Janmey, P. A., J. Peetermans, K. S. Zaner, T. P. Stossel, and T. Tanaka. 1986. Structure and mobility of actin filaments as measured by quasielastic light scattering, viscometry, and electron microscopy. *J. Biol. Chem.* 261:8357–8362.

Jen, C. J., L. V. McIntire, and J. Bryan. 1982. The viscoelastic properties of actin solutions. *Arch. Biochem. Biophys.* 216:126–132.

Joshi, H. C., D. Chu, R. E. Buxbaum, and S. R. Heidemann. 1985. Tension and compression in the cytoskeleton of PC 12 neurites. *J. Cell Biol.* 101: 697–705.

Kasai, M., H. Kawashima, and F. Oosawa. 1960. Structure of F-actin solutions. *J. Polym. Sci. Part D Macromol. Rev.* 44:51–69.

Koppel, D. E., D. Axelrod, J. Schlessinger, E. L. Elson, and W. W. Webb. 1976. Dynamics of fluorescence marker concentration as a probe of mobility. *Biophys. J.* 16:1315–1329.

Lacowicz, J. R. 1983. Principles of Fluorescence Spectroscopy. Plenum Publishing Corp., New York. 153 pp.

Lekkerkerker, H. N. W., Ph. Coulon, R. Van Der Haegen, and R. Deblieck. 1984. On the isotropic-liquid crystal phase separation in a solution of rodlike particles of different length. *J. Chem. Phys.* 80:3427–3433.

MacLean-Fletcher, S., and T. D. Pollard. 1980. Identification of a factor in

conventional muscle actin preparations which inhibits actin filament self-association. *Biochem. Biophys. Res. Commun.* 86:18-27.

Martin, A. N., J. Swarbrick, and A. Cammarata. 1983. Physical Pharmacy: Physical Principles in the Pharmaceutical Sciences. Lea and Febiger, Philadelphia, Pennsylvania. 543 pp.

Maruyama, K., M. Kaibara, and E. Fukada. 1974. Rheology of F-actin. I. Network of F-actin in solution. *Biochim. Biophys. Acta.* 371:20-29.

Onsager, L. 1949. The effects of shape on the interaction of colloidal particles. *Ann. NY Acad. Sci.* 51:627-659.

Oosawa, F., and S. Asakura. 1975. Theory of polymerization equilibrium. *In* Thermodynamics of the Polymerization of Protein. Academic Press Inc., New York. 25-40.

Petersen, N. O., S. Felder, and E. L. Elson. 1986. Measurement of lateral diffusion by fluorescence photobleaching recovery. *In* Handbook of Experimental Immunology. Vol. 1. Immunochemistry. D. M. Weir, L. A. Herzenberg, C. Blackwell, and L. A. Herzenberg, editors. Blackwell Scientific Publications, Oxford. 24.1-24.23.

Petersen, N. O., W. B. McConnaughey, and E. L. Elson. 1982. Dependence of locally measured cellular deformability on position on the cell, temperature, and cytochalasin B. *Proc. Natl. Acad. Sci. USA.* 79:5327-5331.

Pollard, T. D., and J. A. Cooper. 1982. Methods to characterize actin filament networks. *Methods Enzymol.* 85:211-233.

Sato, M., G. Leimbach, W. H. Schwarz, and T. D. Pollard. 1985. Mechanical properties of actin. *J. Biol. Chem.* 260:8585-8592.

Sato, M., W. H. Schwarz, and T. D. Pollard. 1986. *Acanthamoeba* profilin affects the mechanical properties of nonfilamentous actin. *J. Biol. Chem.* 261:10701-10706.

Sato, M., W. H. Schwarz, and T. D. Pollard. 1987. Dependence of the mechanical properties of actin/α-actinin gels on deformation rate. *Nature (Lond.).* 325:828-830.

Sato, M., T. Z. Wong, and R. D. Allen. 1983. Rheological properties of living cytoplasm: endoplasm of *Physarum* plasmodium. *J. Cell Biol.* 97:1089-1097.

Sato, M., T. Z. Wong, D. T. Brown, and R. D. Allen. 1984. Rheological properties of living cytoplasm: a preliminary investigation of squid axoplasm (Loligo pealei). *Cell Motil.* 4:7-23.

Schmid-Schoenbein, H., R. Wells, and R. Schildkraudt. 1969. Microscopy and viscometry of blood flowing under uniform shear rate (rheoscopy). *J. Appl. Physiol.* 26:674-678.

Singer, R. H., and J. A. Pudney. 1984. Filament-directed intercellular contacts during differentiation of cultured chick myoblasts. *Tissue & Cell.* 16:17-29.

Soua, Z., F. Porte, M.-C. Harricane, J. Feinberg, and J.-P. Capony. 1985. Bovine serum brevin. Purification by hydrophobic chromatography and properties. *Eur. J. Biochem.* 153:275-287.

Spudich, J. A., and S. Watt. 1971. The regulation of rabbit skeletal muscle contraction. I. Biochemical studies of the interaction of the tropomyosin-troponin complex with actin and the proteolytic fragments of myosin. *J. Biol. Chem.* 246:4866-4871.

Stossel, T. P. 1986. The actin system and the rheology of the peripheral cytoplasm. *Biorheology.* 23:621-631.

Stossel, T. P., P. A. Janmey, and K. S. Zaner. 1987. The cortical cytoplasmic actin gel. *In* Cytomechanics. The Mechanical Basis of Cell Form and Structure. J. Bareiter-Hahn, O. R. Anderson, and W.-E. Reif, editors. Springer-Verlag, New York. 131-153.

Tait, J. F., and C. Frieden. 1982a. Polymerization-induced changes in the fluorescence of actin labeled with iodoacetamidotetramethylrhodamine. *Arch. Biochem. Biophys.* 216:133-141.

Tait, J. F., and C. Frieden. 1982b. Polymerization and gelation of actin studied by fluorescence photobleaching recovery. *Biochemistry.* 21:3666-3674.

Taylor, D. L., J. S. Condeelis, P. L. Moore, and R. D. Allen. 1973. The contractile basis of amoeboid movement. I. The chemical control of motility in isolated cytoplasm. *J. Cell Biol.* 59:378-394.

Tellam, R., and C. Frieden. 1982. Cytochalasin D and platelet gelsolin accelerate actin polymer formation. A model for regulation of the extent of actin polymer formation *in vivo. Biochemistry.* 21:3207-3214.

Weihing, R. R. 1985. The filamins: properties and functions. *Can. J. Biochem. Cell Biol.* 63:397-413.

Wells, R. E., Jr., R. Denton, and E. W. Merril. 1961. Measurement of viscosity of biological fluids by cone plate viscometer. *J. Lab. Clin. Med.* 57:646-656.

Zaner, K. S. 1986. The effect of the 540-kilodalton actin cross-linking protein, actin-binding protein, on the mechanical properties of F-actin. *J. Biol. Chem.* 261:7615-7620.

Zaner, K. S., and T. P. Stossel. 1982. Some perspectives on the viscosity of actin filaments. *J. Cell Biol.* 93:987-991.

Zaner, K. S., and T. P. Stossel. 1983. Physical basis of the rheological properties of F-actin. *J. Biol. Chem.* 258:11004-11009.